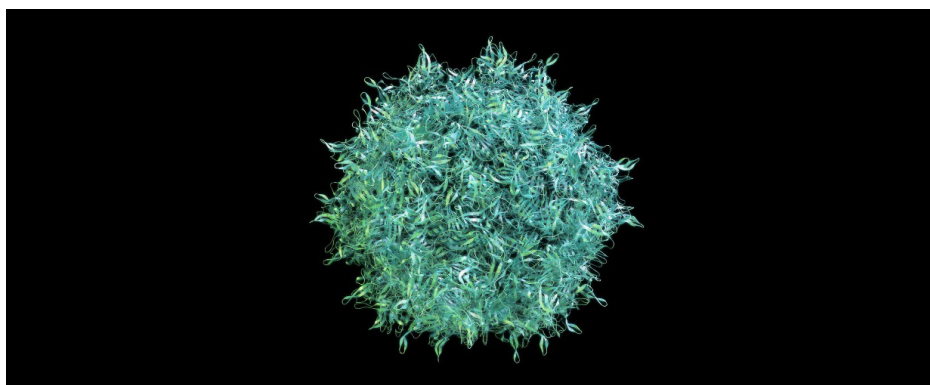


Improved Wide Pore Size Exclusion Chromatography Columns for AAV Analysis

Method development using analytical LC instrumentation



Authors

Andrew Coffey, Charu Kumar,
Ta-Chen Wei, and
Anne Blackwell
Agilent Technologies, Inc.

Abstract

Adeno-associated virus (AAV) particles are an emerging class of biotherapeutic molecule. They are relatively small, approximately 20 to 25 nm in size, but can carry a nucleotide payload of approximately 4,500 bases. They are nonpathogenic and exist in nature as different serotypes with some serotypes having selectivity to target specific organs in the human body. They are therefore extremely useful as vectors for targeted delivery of cell and gene therapies. However, as with all biotherapeutic molecules, product- or process-related impurities are inevitable and must be characterized. Aggregation is one of the most likely critical quality attributes and is best measured using size exclusion chromatography.

Introduction

AAVs are icosahedral structures formed from three related capsid proteins, VP1, VP2, and VP3 (in a ratio of 1:1:10). Approximately 60 capsid proteins form an "empty" AAV particle of approximately 3,700 kDa, or 4,750 kDa as a "full" particle (containing the genomic payload).

As with all protein molecules, AAVs will undergo aggregation under stress conditions, particularly when the concentration is too high.¹

Size exclusion chromatography is an ideal method for measuring aggregation as it can be carried out under non-denaturing conditions. It is important to choose a column with a pore size appropriate for the size of molecule being separated. If there are AAVs with a diameter of 20 to 25 nm, the ideal pore size is 500 Å.

Different serotypes, formed from different capsid proteins, present different structures on the surface of the AAV, which gives the specificity to different organs. This also makes analysis more challenging and the need to optimize method conditions for different serotypes may be necessary.

Experimental

Reagents and chemicals

All reagents were HPLC grade or higher.

Equipment and materials

The following AAV full capsid samples were bought from Charles River Laboratories:

- AAV1, 3.42×10^{11} GC/mL
- AAV2, 1.27×10^{13} GC/mL
- AAV8, 3.53×10^{11} GC/mL
- AAV9, 6.07×10^{11} GC/mL

These samples were stored in PBS + 0.001% pluronic buffer.

Instrumentation

Data acquisition was performed on an Agilent 1260 Infinity II Bio-inert LC system, or an Agilent 1290 Infinity II Bio LC system with Binary High-Speed Pump, as indicated.

Calibration with individual PEG and PEO standards (part number PL2070-0100 and PL2080-0101) required the use of a refractive index detector (RID), an Agilent 1260 Infinity II RID (G7162A).

Analysis of a protein standard (AdvanceBio SEC 300 Å Protein Standard, part number 5190-9417) required the use of a UV detector, an Agilent Infinity II MWD (G7165A).

Analysis of AAV standards required the use of a fluorescence detector (FLD), an Agilent 1260 Infinity II FLD (G7121A).

Sample preparation

Samples were dissolved in the mobile phase, unless already in solution.

Method conditions

HPLC Conditions	
Column	Agilent AdvanceBio SEC 500 Å 2.7 µm, 4.6 × 300 mm (part number PL1580-5325) Agilent AdvanceBio SEC 500 Å 2.7 µm, 4.6 × 150 mm (part number PL1580-3325)
Mobile Phase	For PEG/PEO calibration (Infinity II 1260 Bio-inert): water For protein standard (Infinity II 1260 Bio-inert): 150 mM sodium phosphate, pH 7.0 For method development (Infinity II 1260 Bio-inert): Eluent A: 0.5 M sodium phosphate, pH 7.0 Eluent B: 0.5 M NaCl Eluent C: 0.1 M MgSO ₄ Eluent D: water For AAV serotype analysis (Infinity II 1290 Bio): 50 mM sodium phosphate + 400 mM NaCl, pH 7.2
Flow Rate	0.35 mL/min
Column Temperature	25 °C
Injection Volume	5 µL
Detection	PEG/PEO – RI Proteins – UV, 220 nm AAVs – FLD, λ _{ex} 280 nm, λ _{em} 348 nm

Results and discussion

Initial experiments were undertaken to verify lot-to-lot reproducibility for the 500 Å pore size stationary phase required for optimum size exclusion separation of AAVs (20 to 25 nm in diameter).

Complete characterization of the pore size and pore size distribution can be accomplished in several ways, but chromatographic analysis gives the most appropriate results. This characterization is achieved by calibration with individual polymer standards using different molecular weight PEGs and PEOs across the entire resolving range of the column.

The calibration curve is created by plotting Log(MW) against retention time, and is shown in Figure 1. The three lots used show exceptionally good reproducibility of the pore size and pore size distribution, but it is important to check other molecules too. Proteins contain a wide range of surface features including hydrophobic patches, or areas of concentrated charge from amino acid side chains. These

features can lead to nonspecific interactions between the analyte and the stationary phase, which typically result in broader peaks and increased tailing (and loss of resolution), or late elution.

Figure 2 shows the use of a protein standard mixture where the largest component present is thyroglobulin (including both monomer, peak 2, and dimer, peak 1).

As expected, the protein separation is similar, suggesting no undesirable nonspecific interactions due to the hydrophilic coating of the AdvanceBio SEC stationary phase.

Lack of availability of proteins of very high molecular weight means that the standard does not cover the entire resolving range of the column.

Owing to the difference in characteristics of the various AAV serotypes, it is recommended to explore a variety of method conditions to ensure reproducible results. AAV production is rather low yielding with low concentrations often preferred to avoid issues with aggregation, but this often makes UV detection difficult.

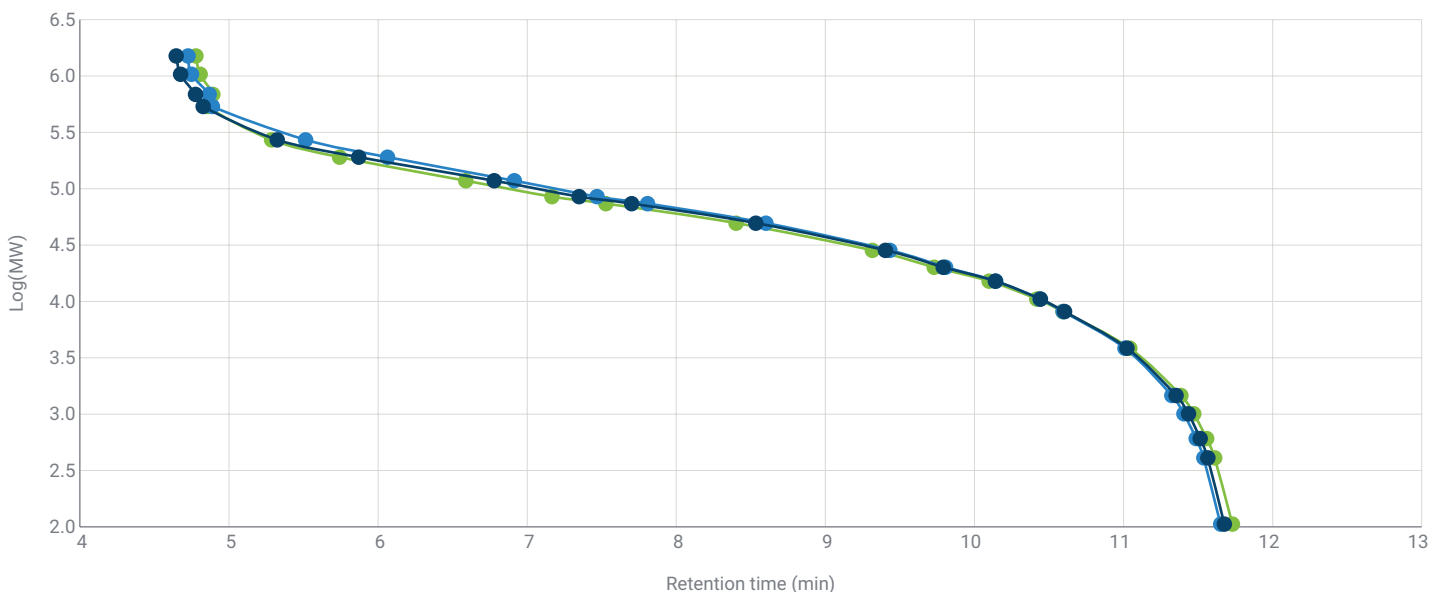


Figure 1. Overlay of PEG/PEO calibration curves for three different lots of Agilent AdvanceBio SEC 500 Å using 4.6 × 300 mm columns on an Agilent 1260 Infinity II Bio LC.

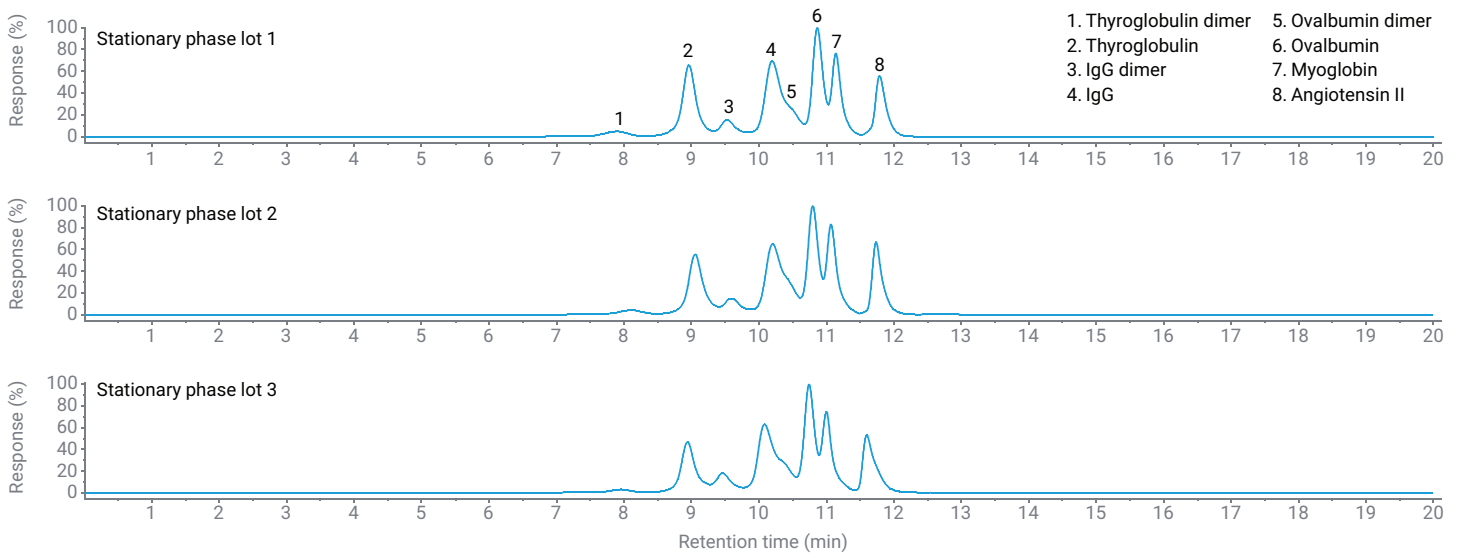


Figure 2. Overlay of protein standards for three different lots of Agilent AdvanceBio SEC 500 Å using 4.6 × 300 mm columns on an Agilent 1260 Infinity II Bio LC.

Figures 3A and 3B show a comparison between the response from an FLD detector and the response from a UV detector at 220 nm (i.e., the most sensitive wavelength). In the zoomed in chromatogram (Figure 3B), the signal-to-noise ratio is much lower with the UV detector at 220 nm than with the FLD detector. The FLD is picking up a small amount of AAV2 aggregate (at approximately 6.8 minutes) that is missing in the UV trace. Furthermore, there is a large peak at 11.7 minutes that is due to the formulation of the sample. It may be due to a preservative or other component that absorbs strongly at 220 nm.

Mobile phase optimization should include choice of buffer, buffer concentration, pH, as well as choice of salt and salt concentration. Other additives may also be considered.

In this application note, we chose to focus on sodium phosphate at pH 7.0 for the buffer, exploring the effect of different concentrations, together with differing amounts of sodium chloride.

Including magnesium salts was also investigated since divalent cations are known to stabilize AAV structures and inhibit aggregation.

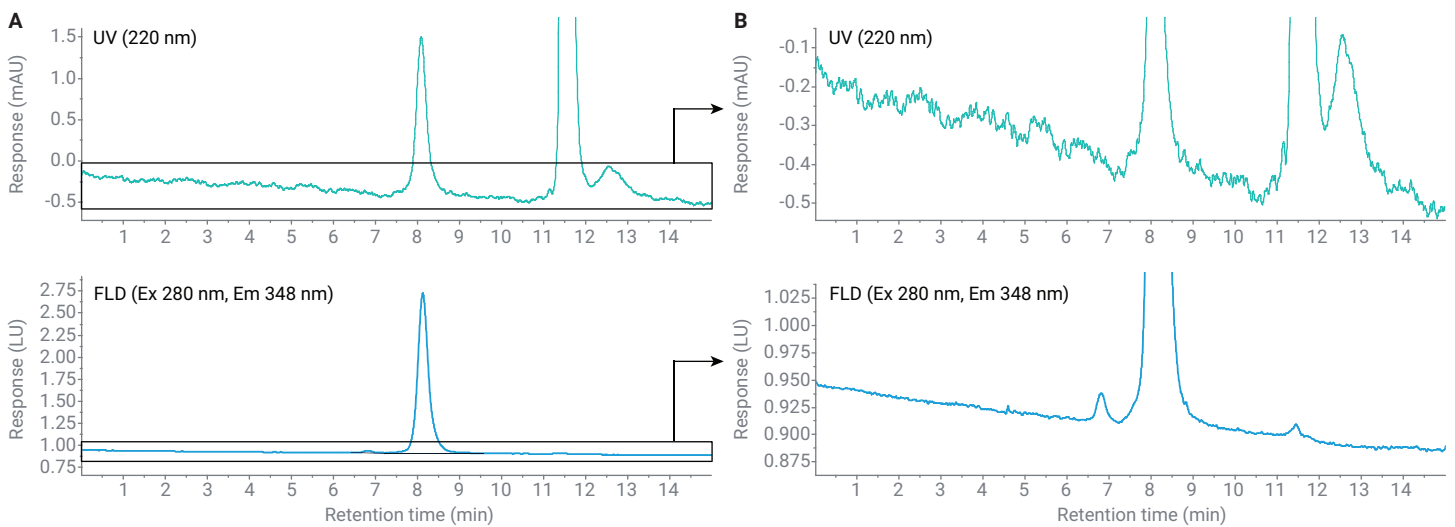


Figure 3. Comparison between UV and fluorescence detection for AAV2 using a 4.6 × 300 mm column on an Agilent 1290 Infinity II Bio LC. (A) Full chromatograms; (B) zoomed-in.

To determine the most suitable mobile phase composition for AAV8 analysis, a series of experiments was run using the Infinity II 1260 Bio-inert LC instrument. The quaternary pump gave the possibility of blending the necessary components together to explore many mobile phase solutions. By mixing different proportions of eluents shown in the method conditions, mobile phase solutions of 25 and 50 mM sodium phosphate buffer, 100, 200, 300, and 400 mM NaCl, and 0 or 5 mM magnesium sulfate were tested.

The chromatograms were analyzed and with particular attention paid to the dimer area%, resolution, and peak tailing.

Table 1 shows the combinations of mobile phase and Figures 4 and 5 illustrate the consistency in peak resolution and tailing throughout the experiment.

Table 1. Summary of method optimization experiments.

Experiment Number	%A	%B	%C	%D	NaPO (mM)	NaCl (mM)	MgSO ₄ (mM)
1	5%	20%	0%	75%	25	100	0
2	5%	40%	0%	55%	25	200	0
3	5%	60%	0%	35%	25	300	0
4	5%	80%	0%	15%	25	400	0
5	10%	20%	0%	70%	50	100	0
6	10%	40%	0%	50%	50	200	0
7	10%	60%	0%	30%	50	300	0
8	10%	80%	0%	10%	50	400	0
9	5%	20%	5%	70%	25	100	5
10	5%	40%	5%	50%	25	200	5
11	5%	60%	5%	30%	25	300	5
12	5%	80%	5%	10%	25	400	5
13	10%	20%	5%	65%	50	100	5
14	10%	40%	5%	45%	50	200	5
15	10%	60%	5%	25%	50	300	5
16	10%	80%	5%	5%	50	400	5

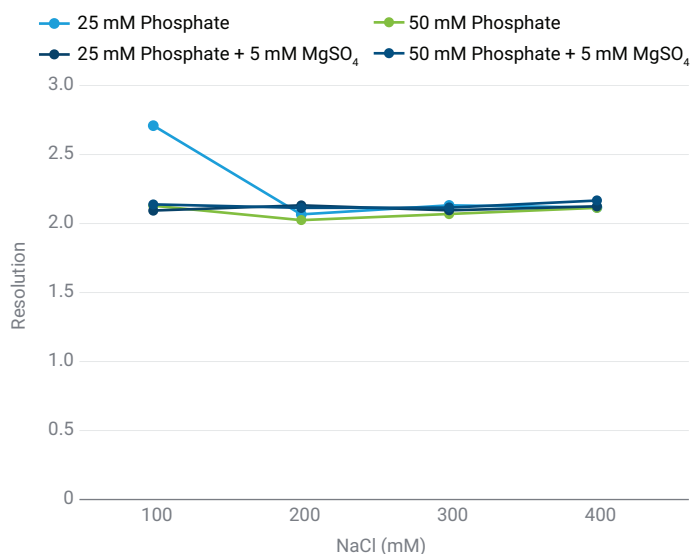


Figure 4. Monomer-dimer resolution observed during method optimization using a 4.6 × 300 mm column on an Agilent 1260 Infinity II Bio-inert LC.

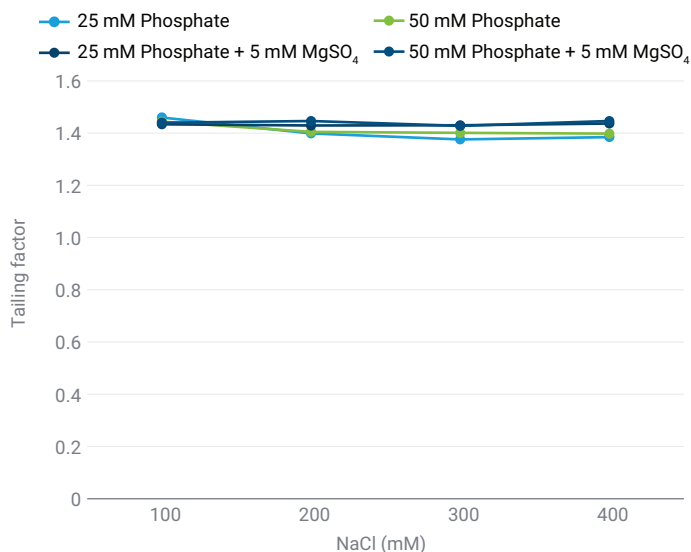


Figure 5. AAV8 Monomer peak tailing observed during method optimization using a 4.6 × 300 mm column on an Agilent 1260 Infinity II Bio-inert LC.

The first experiment at the lowest ionic strength of just 25 mM sodium phosphate + 100 mM NaCl gave an artificially high resolution between the monomer and dimer peaks. This was due to inaccurate analysis of a very low recovery dimer peak.

The most consistent results for AAV8 were obtained using a sodium phosphate concentration of 50 mM. Higher levels of NaCl were also beneficial.

Next, columns from three different lots of stationary phase were compared. Samples of AAV1 (Figure 6A), AAV8 (Figure 6B), and AAV9 (Figure 6C) were analyzed and the results were compared (Figure 6D).

Excellent lot-to-lot reproducibility was observed using the Infinity II 1290 Bio LC system.

Further investigation looked at run-to-run reproducibility of a fourth serotype, AAV2 on one of the columns.

Figure 7A shows the results from four separate runs, with a zoomed in view shown in Figure 7B.

With average dimer area% of 1.19, resolution of 3.09, and peak tailing of 1.21, all with %RSD < 0.5, the injection-to-injection consistency was also excellent.

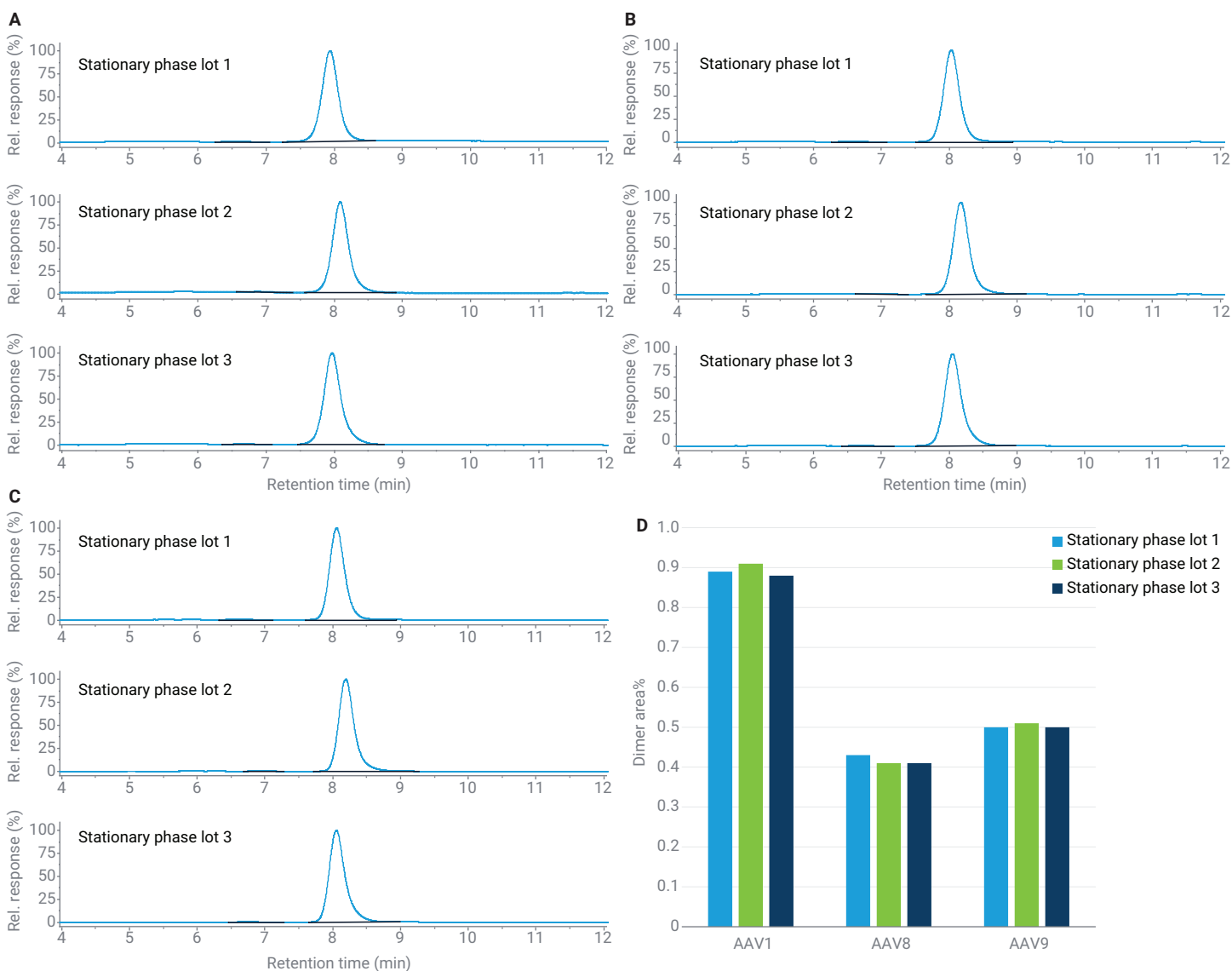


Figure 6. Lot-to-lot comparison (A) AAV1, (B) AAV8, and (C) AAV9 on a 4.6 × 300 mm column using an Agilent 1290 Infinity II Bio LC. The percent area of the dimer peak was consistent from lot to lot (D).

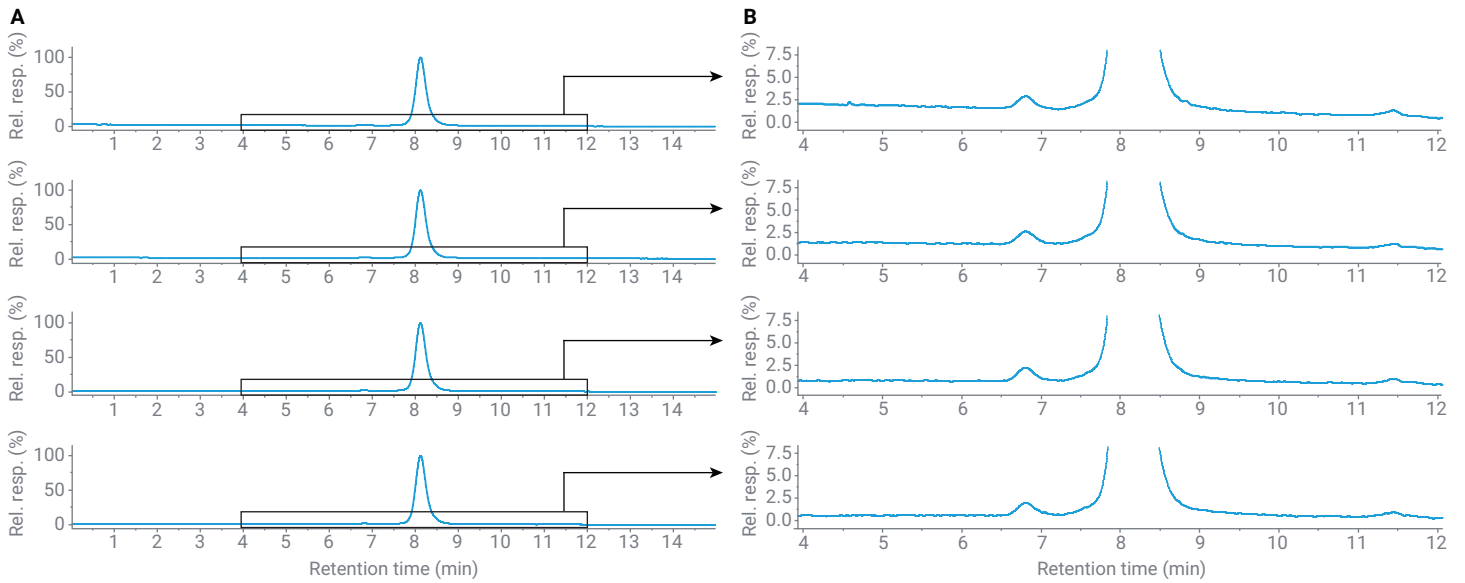


Figure 7. Four replicated injections of AAV2 demonstrating excellent injection-to-injection consistency using a 4.6 × 300 mm column on an Agilent 1290 Infinity II Bio LC. (A) Full chromatograms; (B) zoomed-in.

The final part of this investigation was to evaluate the performance of a shorter 150 mm column. The reduced column volume means that the run time is cut by 50%, but a lower resolution is to be expected. A fresh AAV8 sample was prepared and analyzed using an Infinity II 1290 LC instrument. The results are shown in Figure 8, with excellent resolution for

peak area on both columns. Despite the expected reduction in resolution, an R_s value of 2.1 is still sufficient to provide confidence in the dimer peak area% measurement, but with much higher throughput. The dimer percent area measured was unchanged with the shorter analysis combined with low dead volume on the 1290 Infinity II Bio LC.

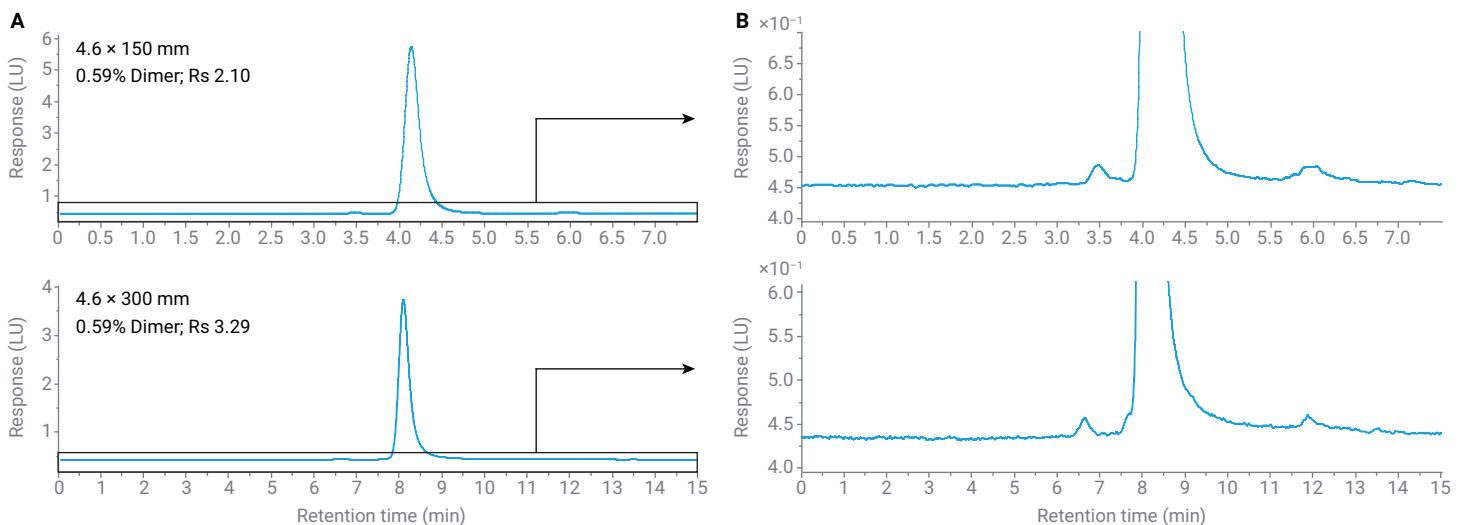


Figure 8. AAV8 injection on 4.6 × 150 mm (top) and 4.6 × 300 mm (bottom) column dimensions using an Agilent 1290 Infinity II Bio LC. (A) Full chromatograms; (B) zoomed-in.

Conclusion

This application note demonstrates the excellent lot-to-lot reproducibility of the new AdvanceBio SEC 500 Å for the analysis of AAV aggregation in many serotypes.

The combination of wide pore size, high pore volume, and optimal particle size means that column performance is not compromised, even when choosing shorter 150 mm columns for higher throughput.

Reference

1. Qu, G.; *et al.* Evidence That Ionic Interactions Are Involved in Concentration-Induced Aggregation of Recombinant Adeno-Associated Virus. *Mol. Therapy* (May **2003**), *7*(5), S348.



031 336 90 00 • www.scantecnordic.se

www.agilent.com

DE18634281

This information is subject to change without notice.

© Agilent Technologies, Inc. 2024
Printed in the USA, May 28, 2024
5994-7509EN

